Gas-Phase Ionic Syntheses of Amino Acids: β versus α

Jamie L. Snow,[†] Galina Orlova,[*,†] Voislav Blagojevic,[‡] and Diethard K. Bohme[*,‡]

Contribution from the Department of Chemistry, St. Francis Xavier University, Antigonish, Nova Scotia, Canada B2G 2W5, and Department of Chemistry and Centre for Research in Mass Spectrometry, York University, 4700 Keele Street, Toronto, Ontario, Canada M3J 1P3
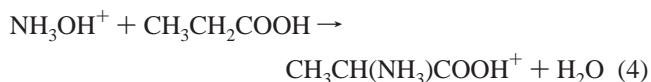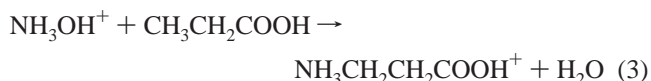
Received December 5, 2006; E-mail: gorlova@stfx.ca; dkbohme@yorku.ca

Abstract: Both theoretical and experimental studies are reported for the gas-phase reactions of protonated hydroxylamine with acetic and propanoic acids which yield protonated glycine and alanine, GlyH$^+$ and AlaH$^+$, respectively. The key step for these reactions is an insertion of the amino group into a C−H bond. For the formation of AlaH$^+$, the reaction barrier for insertion into a C$_\beta$−H bond is ca. 5 kcal·mol^{-1} lower than that for the insertion into a C$_\alpha$−H bond; the product β-AlaH$^+$ is ca. 6 kcal mol^{-1} lower in energy than α-AlaH$^+$. Thus, both kinetics and thermodynamics favor formation of the β-form. The energetic preference for the β-form is due to more efficient hydrogen bonding between the amino group and the carbonyl oxygen in the limiting transition structure and in the β-AlaH$^+$ product. These theoretical results are in excellent accord with selected ion flow tube measurements of the gas-phase synthesis which show striking specificity for the β-isomer according to multi-collision-induced dissociation of the AlaH$^+$ product ion. The results suggest that Gly and β-Ala found in carbonaceous chondrite meteorites are products of interstellar chemistry.

Introduction

We have recently demonstrated, using both experiment and theory,[1,2] that the gas-phase hydrolysis of ionized ketene, H$_2$C= C=O$^{\bullet+}$, yields acetic acid and that carboxylic acids could be formed on icy surfaces in hot cores and interstellar clouds. Carboxylic acids, in turn, are precursors for the formation of amino acids: the gas-phase reactions between protonated hydroxylamine and acetic or propanoic acid yield protonated glycine or alanine, respectively.[2] These amino acids are building materials for more complex biomolecules.[3] Several amino acids, Gly, Ala, and γ-aminobutyric acid, have been found in carbonaceous chondrite meteorites (CMs).[4] Some authors have suggested that the organic compounds of CMs could be formed abiotically in the interstellar media and might have been delivered to the early Earth.[5,6] The most abundant amino acid found in CMs is β-alanine (40%), which exceeds the percentage of the α-form by a factor of 9.[4] Preliminary results of flow reactor/tandem mass spectrometer experiments in the Bohme group[2] showed that, indeed, the gas-phase reaction between propanoic acid and protonated hydroxylamine yields predominantly a β-form of protonated alanine. No α-form was detected. The reaction mechanism and the reason for this striking specificity for the β-form remained unclear.

Here we report the detailed theoretical and experimental studies of reaction mechanisms for the formation of protonated hydroxylamine, NH$_3$OH$^+$, by reaction 1 and protonated amino acids GlyH$^+$ by reaction 2, β-AlaH$^+$ by reaction 3, and α-AlaH$^+$ by reaction 4.

$$CH_5^+ + NH_2OH \rightarrow CH_4 + NH_3OH^+ \tag{1}$$

$$NH_3OH^+ + CH_3COOH \rightarrow NH_3CH_2COOH^+ + H_2O \tag{2}$$

$$NH_3OH^+ + CH_3CH_2COOH \rightarrow$$
$$NH_3CH_2CH_2COOH^+ + H_2O \tag{3}$$

$$NH_3OH^+ + CH_3CH_2COOH \rightarrow$$
$$CH_3CH(NH_3)COOH^+ + H_2O \tag{4}$$

Methods

1. Computational Details. All theoretical predictions were made with the GAUSSIAN03 package.[7] Density functional theory was employed to determine optimized geometries, energetics, and atomic charges. The B3LYP functional with Becke's three-parameter hybrid exchange, B3,[8] and the correlation functional of Lee, Yang, and Parr, LYP,[9] was used predominantly. Several other exchange-correlation functionals were tested for the comparison: the meta-GGA functionals VSXC[10] (Voorhis and Scuseria's τ-dependent gradient-corrected exchange-correlation functional) and HCTH/407[11,12] (Handy's exchange-

[†] St. Francis Xavier University.
[‡] York University.
(1) Orlova, G.; Blagojevic, V.; Bohme, D. K. *J. Phys. Chem. A* **2006**, *110*, 8266.
(2) Blagojevic, V.; Petrie, S.; Bohme, D. K. *Mon. Not. R. Astron. Soc.* **2003**, *339*, L7−L11.
(3) Wincel, H.; Fokkens, R. H.; Nibbering, N. M. M. *Rapid Commun. Mass Spectrom.* **2000**, *14*, 135.
(4) Ehrenfreund, P.; Glavin, D. P.; Botta, O.; Cooper, G.; Bada, J. L. *Proc. Natl. Acad. Sci. U.S.A.* **2001**, *98*, 2138.
(5) Engel, M. H.; Mascko, S. A. *Nature* **1997**, *389*, 265.
(6) Pizzarello, S. *Acc. Chem. Res.* **2006**, *39*, 231.

(7) Frisch, M. J.; et al. *Gaussian 03*, revision C.02; Gaussian, Inc.: Wallingford, CT, 2004.
(8) Becke, A. D. *J. Chem. Phys.* **1993**, *98*, 5648.
(9) Lee, C.; Yang, W.; Parr, R. G. *Phys. Rev. B* **1988**, *37*, 785.
(10) Van Voorhis, T.; Scuseria, G. E. *J. Chem. Phys.* **1998**, *109*, 400.
(11) Boese, A. D.; Handy, N. C. *J. Chem. Phys.* **2001**, *114*, 5497.
(12) Boese, A. D.; Doltsinis, N. L.; Handy, N. C.; Sprik, M. *J. Chem. Phys.* **2000**, *112*, 1670.

correlation functional), as well as hybrid functionals BHandHLYP, with 50% of the exact exchange, as implemented in Gaussian03, and B98.[13] The VSXC exchange-correlation functional yields the best agreement with experimental data in thermochemistry, similar to that from B3LYP. Thus, VSXC was used further along with B3LYP for the prediction of the reaction mechanisms. For selected structures, single-point energy calculations were performed with the coupled cluster method, CCSD(T),[14−18] using the B3LYP and VSXC geometries and zero-point vibrational energy corrections.

The triple-ζ 6-311++G(df,pd) basis set[19,20] with diffuse and polarization functions on the heavy and hydrogen atoms[21,22] was used predominantly. Various sets of diffuse and polarization functions for the 6-311G basis set as well as a smaller double-ζ 6-31+G(d) basis set were used for comparison. Harmonic vibrational frequencies were computed to verify minima (all real frequencies) and transition-state structures (one imaginary frequency). The connections between transition states and adjacent minima were verified using the intrinsic reaction coordinate (IRC) technique developed by Gonzalez and Schlegel.[23,24] The visualizations were performed with the GaussViewW software package.[25] All relative energies reported include zero-point vibrational energy corrections.

2. Experimental Details. The flow reactor/tandem mass spectrometer used to study the formation of glycine is a selected ion flow tube (SIFT) instrument that consists of two quadrupole mass filters separated by a steel flow tube.[26] Helium flows through the tube at a constant pressure of 0.35 Torr and room temperature. Ions generated in the ion source are separated by the first quadrupole mass filter before they enter the flow tube upstream, and ions downstream are sampled through a nose cone and analyzed by the second quadrupole mass filter. Electron ionization (EI) and inductively coupled plasma (ICP) ion sources were used in these experiments. Collisions with the buffer gas thermalize the ions derived from the ion source or generated upstream by chemical reaction before they enter the reaction region downstream. CO, methane, and ethylene were added as pure gases, water was added as a 2% mixture of vapor in helium, and the carboxylic acids and hydroxylamine were added as pure vapors of the corresponding solids or liquids.

It is important to note that even though the measurements were made at 0.35 Torr and room temperature, the results should apply to low-pressure, low-temperature environments. The rates of bimolecular ion−molecule reactions are pressure independent and often do not exhibit activation energies because of the electrostatic interaction between ions and molecules. Bimolecular ion−molecule reactions with measurable rate coefficients at room temperature, say $k > 10^{-12}$ cm^3 molecule^{-1} s^{-1}, do not possess an activation barrier more than a few kilocalories per mole above the initial energy of the separated reactants.

Table 1. Reaction Enthalpies, ΔH_0, kcal mol^{-1}, for the Formation of GlyH$^+$ (Reaction 2) Predicted Using Various Computational Methods and Basis Sets

method	ΔH_0
B3LYP/6-31+G(d)	44.6
B3LYP/6-311+G(d)	50.3
B3LYP/6-311+G(df,p)	53.7
B3LYP/6-311++G(df,pd)	54.1
B3LYP/ 6-311++G(3df,3pd)	51.7
CCSD(T)//B3LYP/ 6-311++G(df,pd)	57.3
B98/6-311+G(d)	50.9
BHandH/6-311+G(d)	51.8
VSXC/6-311+G(d)	54.1
VSXC/6-311++G(d,p)	58.0
CCSD(T)//VSXC/ 6-311++G(d,p)	55.6
HCTH407/ 6-311+G(d)	49.1
experiment (see the text)	54.8 ± 3

Bond connectivities within the ions sampled can be explored by changing the nose cone potential[27] and thereby induce multicollisional dissociation (CID). To achieve higher collision energies in CID experiments, argon was used instead of helium at pressures around 0.14 Torr. Whenever possible, the experiments were performed in sequence (synthesized ion/commercial ion) to minimize differences in the experimental conditions.

Results and Discussion

1. Reaction Enthalpies and Performance of Various Exchange-Correlation Functionals. Enthalpies for reactions 2−4 calculated using reference enthalpies of formation and proton affinities (PAs)[28] yield the following exothermicities: 54.8 ± 3 kcal mol^{-1} for GlyH$^+$, 60.5 ± 4 kcal mol^{-1} for α-AlaH$^+$, and 67.9 ± 4 kcal mol^{-1} for β-AlaH$^+$. The details are available in the Supporting Information. Our calculations predict a value for PA(β-Ala) = 221.0 kcal mol^{-1} (the experimental value is 221.6 ± 1 kcal mol^{-1})[28e] using the B3LYP/6-311++G(df, pd) method and a value for PA(α-Ala) = 214.1 kcal mol^{-1} (the experimental value is 215.6 ± 2 kcal mol^{-1}).[28b] The PA of β-Ala is greater than that of α-Ala by 6.9 kcal mol^{-1} apparently due to the more effective N−H$^+$−O hydrogen bridge in β-AlaH$^+$.

The experimental enthalpy (54.8 ± 3 kcal mol^{-1}) for the formation of GlyH$^+$ was used for testing of various exchange-correlation functionals and basis sets. The results are listed in Table 1. The thermal corrections to 298 K are negligibly small (within 0.1 kcal mol^{-1}); thus, only the values at 0 K are reported. DFT exchange-correlation functionals exhibit a strong dependence on the size of the basis set. The commonly used combination of hybrid B3LYP exchange-correlation functional and double-ζ 6-31+G(d) basis set underestimates the exothermicity by ca. 20%. The triple-ζ 6-311++G(df, pd) basis set with B3LYP yields nearly a target value. The single-point energy calculations using the CCSD(T)/6-311++G(df, pd) method with the B3LYP/6-311++G(df, pd) geometries and zero-point vibrational energy correction yield a somewhat greater value within the uncertainty of the experimental value. A further

(13) Schmider, H. L.; Becke, A. D. *J. Chem. Phys.* **1998**, *108*, 9624.
(14) Čizek, J. *Adv. Chem. Phys.* **1969**, *14*, 35.
(15) Purvis, G. D.; Bartlett, R. J. *J. Chem. Phys.* **1982**, *76*, 1910.
(16) Scuseria, G. E.; Janssen, C. L.; Schaefer, H. F., III. *J. Chem. Phys.* **1988**, *89*, 7382.
(17) Scuseria, G. E.; Schaefer, H. F., III. *J. Chem. Phys.* **1989**, *90*, 3700.
(18) Pople, J. A.; Head-Gordon, M.; Raghavachari, K. *J. Chem. Phys.* **1987**, *87*, 5968.
(19) Hehre, W. J.; Ditchfield, R.; Pople, J. A. *J. Chem. Phys.* **1972**, *56*, 2257.
(20) Krishnan, R.; Binkley, J. S.; Seeger, R.; Pople, J. A. *J. Chem. Phys.* **1980**, *72*, 650.
(21) Chandrasekhar, J.; Andrade, J. G.; Schleyer, P. v. R. *J. Am. Chem. Soc.* **1981**, *103*, 5609−5612.
(22) Clark, T.; Chandrasekhar, J.; Spitznagel, G. W.; Schleyer, P. v. R. *J. Comput. Chem.* **1983**, *4*, 294−301.
(23) Gonzalez, C.; Schlegel, H. B. *J. Chem. Phys.* **1989**, *90*, 3154.
(24) Gonzalez, C.; Schlegel, H. B. *J. Phys. Chem.* **1990**, *94*, 5523.
(25) Dennington, R., II; Keith, T.; Millam, J.; Eppinnett, K.; Hovell, W. L.; Gilliland, R. *GaussView*, version 3.09; Semichem, Inc.: Shawnee Mission, KS, 2003.
(26) (a) Mackay, G. I.; Vlachos, G. D.; Bohme, D. K.; Schiff, H. I. *Int. J. Mass Spectrom. Ion Phys.* **1980**, *36*, 259. (b) Raksit, A. B.; Bohme, D. K. *Int. J. Mass Spectrom. Ion Processes* **1983**, *55*, 69. (c) Koyanagi, G. K.; Lavrov, V. V.; Baranov, V.; Bandura, D.; Tanner, S.; McLaren, J. W.; Bohme, D. K. *Int. J. Mass Spectrom.* **2000**, *194*, L1. (d) Koyanagi, G. K.; Baranov, V. I.; Tanner, S. D.; Bohme, D. K. *J. Anal. At. Spectrom.* **2000**, *15*, 1207−1210.

(27) Baranov, V.; Bohme, D. K. *Int. J. Mass Spectrom. Ion Processes* **1996**, *154*, 71.
(28) (a) Ngauv, S. N.; Sabbah, R.; Laffitte, M. *Thermochim. Acta* **1977**, *20*, 371−380. (b) Hunter, E. P.; Lias, S. G. *J. Phys. Chem. Ref. Data* **1998**, *27* (3), 413−656. (c) Sabbah, R.; Skoulika, S. *Thermochim. Acta* **1980**, *36*, 179−187. (d) Cox, J. D.; Wagman, D. D.; Medvedev, V. A. *CODATA Key Values for Thermodynamics*; Hemisphere Publishing Corp.: New York, 1984; p 1. (e) Hahn, I.-S.; Wesdemiotis, C. *Int. J. Mass Spectrom. Ion Processes* **2003**, *222*, 465.
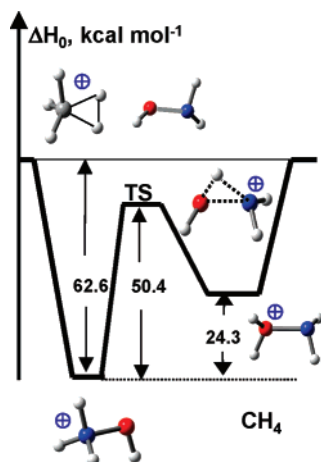
Figure 1. Relative enthalpies at 0 K, ΔH_0, for the formation of two isomers of protonated hydroxylamine from CH_5^+ and NH_2OH, predicted with the B3LYP/6-311++G(df,pd) method.

increase in the flexibility of the basis set with B3LYP causes a decrease in exothermicity within the experimental uncertainty.

The hybrid B98 and BHandH and GGA VSXC and HCTH/407 exchange- correlation functionals were tested for the comparison with B3LYP. With a moderate 6-311+G(d) basis set, B98 and BHandH yield an exothermicity which is slightly below the target value but within the range. HCTH/407 drops the value below the experimental range. The VSXC/6-311+G-(d) method predicts nearly the target value, 54.1 kcal mol^{-1}; the additional set of diffuse and polarization functions on H atoms (6-311++G(d,p)) increases the exothermicity by 3.9 kcal mol^{-1}. The CCSD(T)//VSXC/6-311++G(d,p) value is also in excellent accord with experiment. Thus, the meta-GGA VSXC exchange-correlation functional was used further for the prediction of reaction mechanisms along with the hybrid B3LYP, which is a basic computational method.

2. Protonation of Hydroxylamine. Experimentally, protonation of hydroxylamine in the gas phase was performed using CH_5^+ as a protonating agent. The potential energy profile for the corresponding reaction 1 predicted with the B3LYP/6-311++G(df, pd) method is depicted in Figure 1. The geometries and energetics are available in the Supporting Information. According to B3LYP, a proton migrates from CH_5^+ to the NH_2 group of hydroxylamine without a barrier to form NH_3OH^+. The reaction is strongly exothermic (62.6 kcal mol^{-1}), and this allows a 1,2-proton shift that leads to a higher energy isomer, $NH_2OH_2^+$. The reaction barrier to the shift is below the dissociation limit to NH_2OH and CH_5^+ by 12.2 kcal mol^{-1} and by the same amount on the free energy surface at 298 K. Thus, both NH_3OH^+ and $NH_2OH_2^+$ isomers can be formed in the protonation of NH_2OH by CH_5^+.

3. Reaction of Protonated Hydroxylamine with Acetic Acid: Formation of GlyH$^+$. In the gas-phase experiment, protonated hydroxylamine, NH_3OH^+, possibly with some admixture of the higher energy isomer $NH_2OH_2^+$ is allowed to interact with injected acetic acid to form GlyH$^+$ and a water molecule. The proposed reaction mechanism for GlyH$^+$ formation implies an insertion of the NH_2 group of protonated hydroxylamine into a C–H bond of acetic acid along with N–O bond cleavage; a water molecule leaves the system. The higher energy $NH_2OH_2^+$ isomer already contains H_2O as a leaving group and NH_2 as an insertion group, while the low-energy
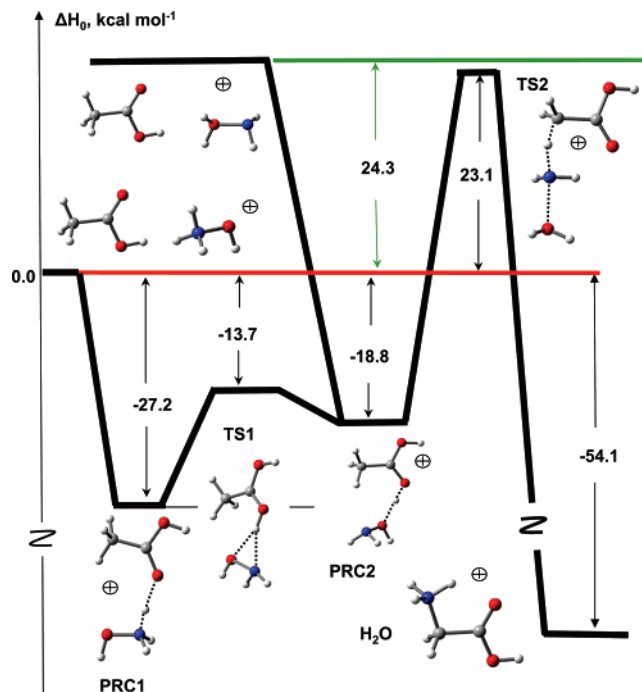

Figure 2. Potential energy profile for the reaction between protonated hydroxylamine and acetic acid to produce GlyH$^+$ predicted with the B3LYP/6-311++G(df,pd) method.

isomer NH_3OH^+ should be rearranged. The potential energy profile predicted for reaction 2 for both isomers using the B3LYP/6-311++G(df,pd) method is shown in Figure 2. The energetics and geometries are available in the Supporting Information.

The low-energy NH_3OH^+ isomer in the initial reaction step forms a prereaction complex, PRC1, with the NH_3 group bound to the carbonyl oxygen of acetic acid via a hydrogen bridge. The formation of PRC1 is 27.2 kcal mol^{-1} exothermic. At the next step, the carbonyl oxygen atom of the acetic acid acts formally as a carrier in the 1,2-proton shift from the nitrogen to the oxygen atom of the hydroxylamine fragment, via transition state TS1, to form an intermediate, PRC2. The intramolecular proton transport[29] drops the barrier to the 1,2-shift dramatically, from 50.4 (Figure 1) to 13.5 kcal mol^{-1}. The PRC2 intermediate can be formed directly upon reaction between the higher energy isomer $NH_2OH_2^+$ and acetic acid.

The PRC2 intermediate leads to the products GlyH$^+$ and water upon insertion of the NH_2 group into a C–H bond and the N–O bond cleavage, which proceed via a concerted mechanism. This is a rate-limiting step in the reaction pathway. The corresponding transition state TS2 is 23.1 kcal mol^{-1} above the dissociation limit to CH_3COOH and NH_3OH^+ but is 1.2 kcal mol^{-1} below the "top" dissociation limit involving the higher energy isomer $NH_2OH_2^+$. The free energy barrier is computed to be 33.8 kcal mol^{-1} at 298 K. The reaction barrier varies with the change in computational method. The CCSD-(T)//B3LYP/6-311++G(df,pd) extrapolation method increases the barrier slightly and places TS2 3.4 kcal mol^{-1} above the top dissociation limit. In contrast, the meta-GGA VSXC exchange-correlation functional with the 6-311++G(d,p) basis set drops the reaction barrier notably, to 11.4 kcal mol^{-1} below

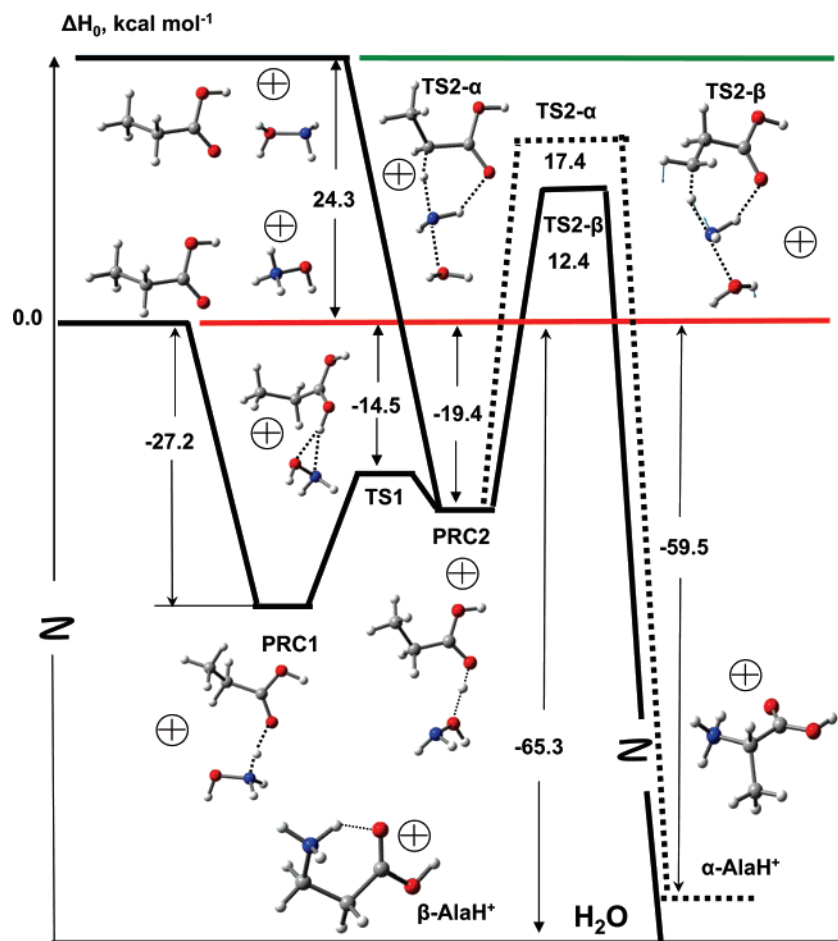(29) Bohme, D. K. *Int. J. Mass Spectrom. Ion Processes* **1992**, *115*, 95.

Figure 3. Potential energy profile for the reaction between protonated hydroxylamine and propanoic acid to produce β-AlaH$^+$ (solid line) and α-AlaH$^+$ (dotted line) predicted with the B3LYP/6-311++G(df,pd) method.

the top limit. However, the CCSD(T)//VSXC/6-311++G(d,p) extrapolation significantly increases the VSXC barrier and predicts TS2 to be 2.2 kcal mol^{-1} above the dissociation limit, similar to the CCSD(T)//B3LYP/6-311++G(df,pd) value. Thus, the VSXC exchange-correlation functional, which predicts an accurate reaction enthalpy, apparently underestimates the reaction barrier, and this is a typical drawback of pure GGA.[30] On the basis of the CCSD(T) and B3LYP results, one can conclude that the limiting barrier on the reaction pathway to the formation of GlyH$^+$ is very close to the dissociation limit to the higher energy reactant NH$_2$OH$_2^+$.

4. Reaction of Protonated Hydroxylamine with Propanoic Acid: Competition between β- and α-AlaH$^+$ Production. The reaction of protonated hydroxylamine and propanoic acid may yield two competitive products: β-AlaH$^+$ (reaction 3) and α-AlaH$^+$ (reaction 4). The potential energy profiles are shown in Figure 3. The energetics and geometries are available in the Supporting Information. The first two steps for the reaction of propanoic acid with NH$_3$OH$^+$ are reminiscent of the reaction with acetic acid. The prereaction complex PRC1 is formed initially, with the NH$_3$ group interacting with the carbonyl oxygen via a hydrogen bridge. In the next step, propanoic acid

(30) (a) Porezag, D.; Pederson, M. R.; Grossman, J. C. *J. Chem. Phys.* **1995**, *102*, 9345. (b) Mitas, L. *Phys. Rev. Lett.* **1997**, *79*, 4353. (c) Patchkovskii, S.; Ziegler, T. *J. Chem. Phys.* **2002**, *116*, 7806. (d) Grüning, M.; Gritsenko, O. V.; Baerends, E. J. *J. Phys. Chem. A* **2004**, *108*, 4459. (e) Becke, A. D. *J. Chem. Phys.* **2005**, *122*, 064101. (f) Dickson, R. M.; Becke, A. D. *J. Chem. Phys.* **2005**, *123*, 111101.
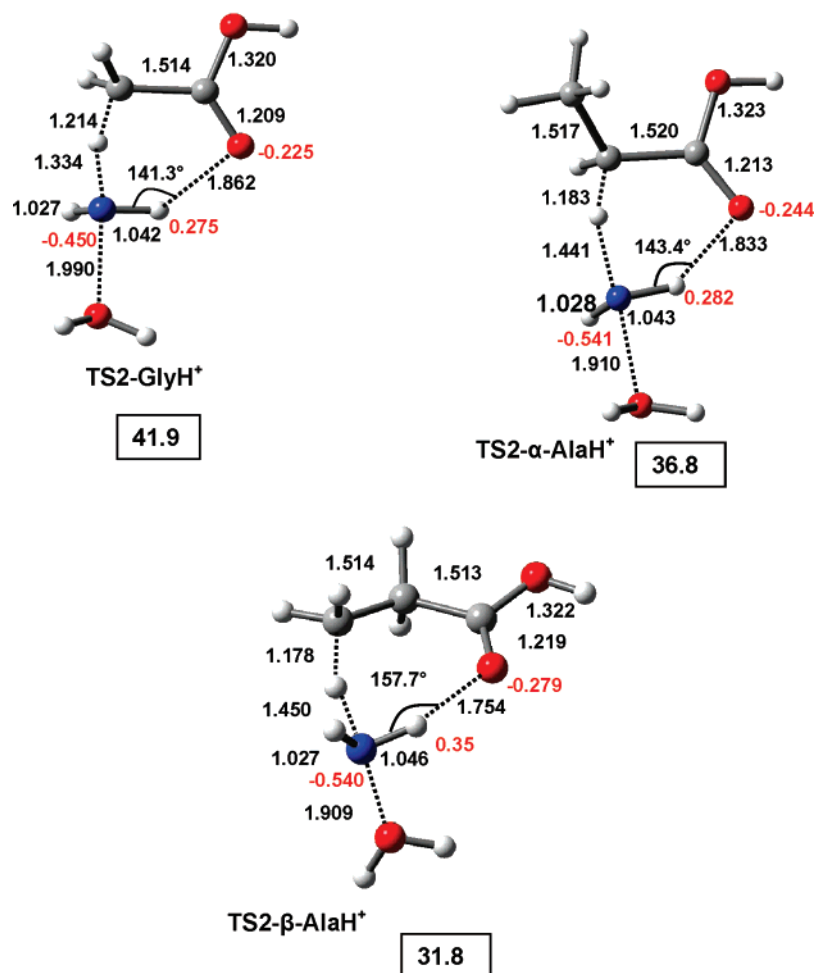
provides efficient proton transport from the NH$_3$ group to OH to form PRC2, with the NH$_2$OH$_2^+$ fragment. The barrier to the 1,2-shift is reduced from 50.4 (Figure 1) to 12.7 kcal mol^{-1}; that is, propanoic acid is a more efficient proton carrier than acetic acid, in accord with the PA values (190.5 and 187.3 kcal mol^{-1}, respectively).[28b] The PRC2 intermediate could be formed directly upon the interaction between propanoic acid and NH$_2$-OH$_2^+$.

The PRC2 intermediate is a loose structure; ethyl rotates about a C$-$C bond via vanishingly small barriers, and the OH$_2$ fragment can recoordinate readily with the carboxylic group oxygens to form nearly degenerate (within 0.5 kcal mol^{-1} at the B3LYP/6-311++G(df,pd) level) isomers. These conformers/isomers lead to different products: α-L-AlaH$^+$, α-D-AlaH$^+$, or β-AlaH$^+$. The PRC2 structure reported in Figure 3 leads to α-L-AlaH$^+$. Other PRC2 forms are not reported for simplicity. The reaction barriers and enthalpies for the formation of L- and D-enantiomers are essentially the same; thus, the α-D-AlaH$^+$ pathway is not reported. Two reaction channels are shown in Figure 3: the NH$_2$ insertion into a C$_\alpha$$-$H bond and into a C$_\beta$$-$H bond to yield α-AlaH$^+$ and β-AlaH$^+$, respectively. Both insertions proceed via a concerted mechanism: the N$-$O bond is broken, and H$_2$O leaves the system. The barrier to a C$_\alpha$$-$H insertion is 5.0 kcal mol^{-1} higher than that to a C$_\beta$$-$H insertion. A similar difference, 4.7 kcal mol^{-1}, is found for the free energy barriers at 298 K (28.2 kcal mol^{-1} for α-AlaH$^+$ and 23.5 kcal mol^{-1} for β-AlaH$^+$).

Figure 4. Selected geometries (Å, deg) for the rate-limiting transition states leading to GlyH$^+$, α-AlaH$^+$, and β-AlaH$^+$ predicted with the B3LYP/6-311++G(df,pd) method. Mulliken charges (red) are reported. The numbers in the boxes show the barrier heights, ΔH_0, kcal mol^{-1}, related to the corresponding PRC2.

The α-AlaH$^+$ product is 5.8 kcal mol^{-1} higher in energy (and 5.4 kcal mol^{-1} higher in free energy) than β-AlaH$^+$. Thus, the formation of the β-form is favored both kinetically and thermodynamically.

The reaction enthalpies predicted with the B3LYP/6-311++G-(df,pd) method, 59.5 and 65.3 kcal mol^{-1} for the α- and β-forms, respectively, are in good accord with the experimental values (60.5 $\pm$ 4 kcal mol^{-1} for α-AlaH$^+$ and 67.9 $\pm$ 4 kcal mol^{-1} for β-AlaH$^+$). The VSXC/6-311++G(d,p) method predicts somewhat greater exothermicities (66.2 and 70.1 kcal mol^{-1}), while the CCSD(T)//VSXC/ 6-311++G(d,p) extrapolation yields nearly the target values (63.9 and 68.4 kcal mol^{-1}).

The rate-limiting reaction barriers for reactions 2−4 relative to the corresponding PRC2 decrease in the following order: 41.9 kcal mol^{-1} (GlyH$^+$), 36.8 kcal mol^{-1} (α-AlaH$^+$), and 31.8 kcal mol^{-1} (β-AlaH$^+$). The former nearly hits the top dissociation limit with B3LYP and even somewhat exceeds the limit with the CCSD(T) extrapolation. To explain the preference for the β-form, the structures of the transition states to β-AlaH$^+$, α-AlaH$^+$, and GlyH$^+$ were analyzed. The selected geometries and relative energetics are shown in Figure 4. The analysis reveals that the reaction barriers decrease when the C−H and N−O bond stretches decrease. The bond stretches Δr_{C-H} and Δr_{N-O} relative to the corresponding PRC2 are as follows: $\Delta r_{C-H} = 0.124$ Å and $\Delta r_{N-O} = 0.557$ Å for TS2-GlyH$^+$, Δr_{C-H}

$= 0.093$ Å and $\Delta r_{N-O} = 0.477$ Å for TS2-α-AlaH$^+$, and $\Delta r_{C-H} = 0.088$ Å and $\Delta r_{N-O} = 0.476$ Å for TS2-β-AlaH$^+$. The lowest TS2-β-AlaH$^+$ is the earliest transition state, while the highest TS2-GlyH$^+$ is the latest one. All three TSs are stabilized with the N−H···O intramolecular hydrogen bond, with the efficacy increasing from TS2-GlyH$^+$ to TS2-β-AlaH$^+$. For TS2-β-AlaH$^+$, the N−H···O moiety has a N−H−O angle (157.7°) closest to linearity, the longest N−H bond, (1.046 Å), and the shortest H···O distance (1.754 Å). The hydrogen bonding causes the elongation of the C=O bond, which is the greatest for TS2-β-AlaH$^+$.

A Mulliken population analysis of the N−H···O moiety reveals the same trend: the positive charge on H and negative charge on O increase on proceeding from TS2-GlyH$^+$ to TS2-β-AlaH$^+$. The H···O population is essentially the same for TS2-GlyH$^+$ and TS2-α-AlaH$^+$ (0.096e) but is slightly higher for TS2-β-AlaH$^+$ (0.113e). We conclude therefore that the earlier onset of the transition state on the reaction pathway to β-AlaH$^+$ is due to more efficient hydrogen bonding, which provides stabilization of 5.0 kcal mol^{-1} compared to the α-form. Nearly the same value, 5.8 kcal mol^{-1}, applies to the stabilization of the β-AlaH$^+$ product compared to α-AlaH$^+$, and they are apparently similar in nature. The H bond provides a six-membered ring for β-AlaH$^+$ and a more strained five-membered ring for the α-form.

5. Experimental Results. Ion−molecule reactions can be especially effective in the synthesis of complex interstellar molecules because the long-range electrostatic interaction between the reactants ensures high reaction efficiency (as it is often sufficient to overcome intrinsic activation energies), even at interstellar temperatures (typically $10-100$ K in molecular environments). In the approach reported here, we have achieved a synthesis of source ions for glycine through ion chemistry using a flow reactor/tandem mass spectrometer instrument that allows the measurement of individual chemical steps in reactions of ions with molecules and concomitantly provides insight into the molecular structure.

The reactions we have identified produce ionized and protonated glycine and involve the reactions of acetic acid with ionized and protonated hydroxylamine produced from hydroxylamine by electron transfer to CO^+ and proton transfer from CH_5^+, respectively. Two major products were observed under our experimental conditions:

$$NH_{2,3}OH^+ + CH_3COOH \rightarrow NH_{2,3}CH_2COOH^+ + H_2O \quad (5a)$$

$$\rightarrow NH_{2,3}OH^+(CH_3COOH) \quad (5b)$$

The rate coefficients for these two reactions are estimated to be $>10^{-12}$ cm^3 molecule^{-1} s^{-1}. The quoted lower limit of 10^{-12} cm^3 molecule^{-1} s^{-1} is derived from an estimate of the amount of carboxylic acid added to the flow tube (precise control of the amount of acid added was not possible because the acid, due to its corrosive nature, interfered with our gas handling and pressure control systems). Elimination of H_2O to form ionized or protonated glycine was observed in about 30% of the reactive collisions, with the remainder leading to collision-stabilized solvation at the He buffer-gas pressure (0.35 Torr) of our experiments. Channel 5a will predominate under interstellar conditions of much lower gas densities at which collisional stabilization becomes negligible, unless radiative association is competitive. The identities of the product ions in channel 5a as ionized and protonated glycine were established in multi-collision-induced dissociation (mCID) experiments in which the observed dissociation of these ions was compared with that observed with commercial glycine ionized by electron transfer to CO^+ or protonated by proton transfer from CH_5^+. Figure 5 shows good agreement not only between the nature of the CID fragment ions but, more importantly, also between the collision energies at which they arise.

The same chemical approach was successful for the synthesis of alanine, using propanoic acid in place of acetic acid:

$$NH_{2,3}OH^+ +$$
$$CH_3CH_2COOH \rightarrow NH_{2,3}CH_2CH_2COOH^+ + H_2O \quad (6a)$$
$$\rightarrow NH_{2,3}OH^+(CH_3CH_2COOH) \quad (6b)$$

The rate coefficients of these two reactions also are estimated to be $>10^{-12}$ cm^3 molecule^{-1} s^{-1}. We have seen that reaction 6a produces ionized or protonated alanine in more than 40% of the reactive collisions under our experimental conditions. Results of mCID experiments show that the β-isomer is produced in reaction 6a rather than the α-isomer. This is illustrated in Figure 6. For the ions derived from the vapors of purchased alanines,
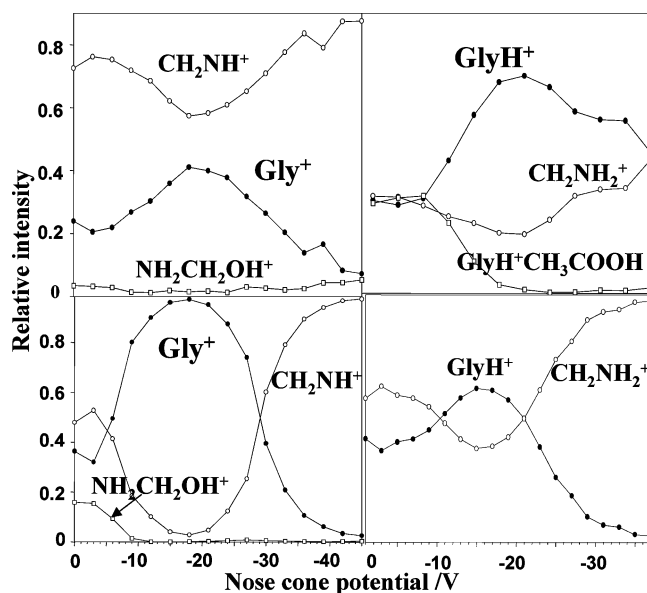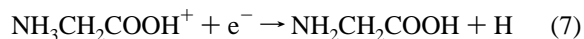

Figure 5. Comparison of mCID profiles of ionized and protonated glycine synthesized in the reactions of $NH_{2,3}OH^+$ with CH_3COOH (top left and right), with ionized and protonated glycine produced from pure glycine vapor (bottom left and right, respectively). Glycine was ionized by electron transfer to CO^+ created in the EI ion source and protonated by proton transfer from the CH_5^+ ion created in the EI ion source from methane. Some $NH_{1,2}CH_2^+$ ions are present initially due to fragmentation of glycine either during ionization and protonation or during vaporization.

the mCID pattern of β-alanine$^+$, $NH_2CH_2CH_2COOH^+$, is distinctly different from that of α-alanine$^+$, $CH_3CH(NH_2)$-$COOH^+$, and is the one that matches the mCID pattern of the ionized product ion in reaction 6a. Most of all, the absence of $CH_3CHNH_2^+$ in the CID profile in Figure 6 of the synthesized β-alanine$^+$ shows that α-alanine$^+$ is not being formed.

Similarly, we have found a match between the mCID profiles of the protonated product ion of reaction 6a and the mCID profile of commercial β-alanine protonated with CH_5^+. Again, the absence of $CH_3CHNH_3^+$ in the CID profile of the synthesized β-alanine-H$^+$ shows that α-alanine-H$^+$ is not being formed.

Plausible interstellar pathways to the neutral amino acids glycine and β-alanine from the ions produced in reactions 5a and 6a involve dissociative recombination, e.g., reaction 7, and electron transfer, e.g., reaction 8,

$$NH_3CH_2COOH^+ + e^- \rightarrow NH_2CH_2COOH + H \quad (7)$$

$$NH_2CH_2COOH^+ + M \rightarrow NH_2CH_2COOH + M^+ \quad (8)$$

where M is a species of lower ionization energy (such as a metal atom) than that of the amino acid itself (for example, IE(gly) $= 8.9$ eV).[28b] Of these processes, the dissociative recombination pathway (reaction 7) is expected to be of greater interstellar significance than reaction 8, since the very high proton affinity of glycine (PA $= 211.6$ kcal mol^{-1}) strongly suggests that no major competing neutralization processes (such as proton transfer to other interstellar molecules) exist for loss of protonated glycine, while the metal atoms thought necessary for reaction 8 are generally considered to be of very low

(31) Adams, N. G.; Herd, C. R.; Geoghegan, M.; Smith, D.; Canosa, A.; Gomet, J. C.; Rowe, B. R.; Queffelec, J. L.; Morlais, M. *J. Chem. Phys.* **1992**, *94*, 4852.
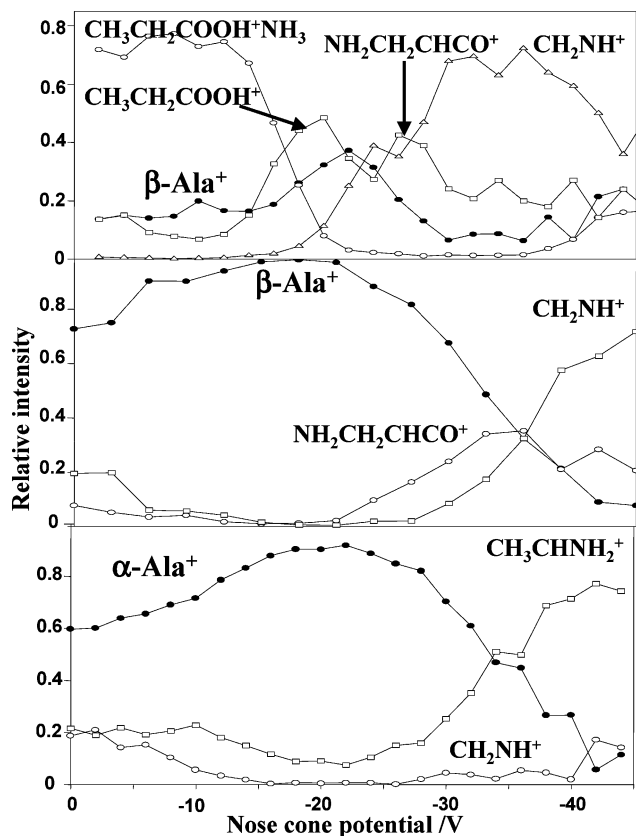
Figure 6. Comparison of mCID profiles of β-alanine cation synthesized in the reaction of NH_2OH^+ with CH_3CH_2COOH (top), ionized β-alanine (middle), and ionized α-alanine (bottom). The latter two ions were produced from β- or α-alanine vapor by electron transfer to CO^+. Some CH_2NH^+ and $NH_2CH_2CHCO^+$ ions are present initially due to fragmentation of β-alanine cations in the process of their formation. The large $CH_3CH_2COOH^+NH_3$ signal present initially arises from the ionization of residual CH_3CH_2COOH reactant by CO^+ (used to ionize NH_2OH) followed by addition of NH_3 (produced in the vaporization of the hydroxylamine hydrochloride). The NH_3 is detached at low nose cone potentials. The rise of β-alanine$^+$ at ~-15 V is due to fragmentation of various weak adducts of β-alanine$^+$ formed with neutral molecules present in the flow tube reactor. These are not shown for clarity. The $NH_2CH_2CHCO^+$ arises from the dissociation of β-alanine$^+$ (there is some mass overlap with $CH_3CH_2COOH^+$ at the resolution employed in the experiments).

abundance in the interstellar regions in which amino acid synthesis is feasible. Although the prediction of the occurrence of the dissociative recombination product channel (reaction 7) is speculative, the small set of protonated molecules for which precise experimental dissociative recombination branching ratios have been reported (H_3O^+, CH_5^+, $C_2H_3^+$, $HCNH^+$) all show that single H atom loss (such as in reaction 7) is a significant product channel.[31]

6. Peptide Bond Formation. Further reaction of glycine synthesized in reaction 5a with acetic acid can lead to formation of *N*-acetylglycine, a compound containing the peptide bond according to reaction 9.
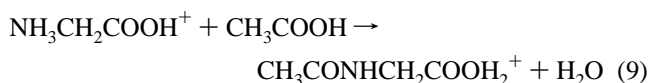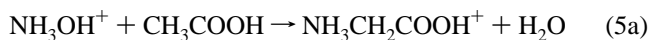
$$NH_3OH^+ + CH_3COOH \rightarrow NH_3CH_2COOH^+ + H_2O \quad (5a)$$

$$NH_3CH_2COOH^+ + CH_3COOH \rightarrow$$
$$CH_3CONHCH_2COOH_2^+ + H_2O \quad (9)$$

Figure 7 shows a comparison between the protonated *N*-acetylglycine synthesized by the ion–molecule reaction and that
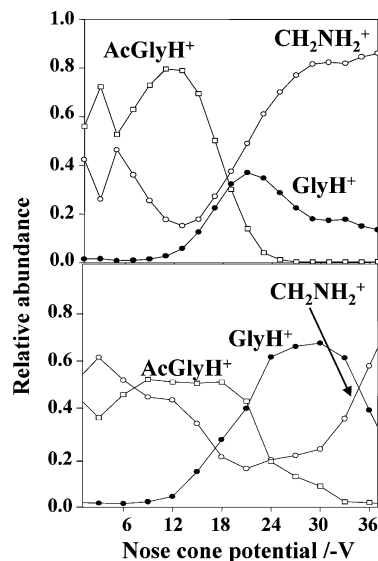

Figure 7. CID profiles for the *N*-acetylglycine synthesized in the reaction of protonated hydroxylamine and acetic acid (top) and protonated *N*-acetylglycine (bottom) created by proton transfer from the H_3O^+ ion created in the reaction of the H_2O^+ ion with water. Water ions were created by electron transfer to Ar^+ ions created in the ICP ion source. The onsets for the dissociation of protonated *N*-acetylglycine ($AcGlyH^+$) and its fragment corresponding to protonated glycine ($GlyH^+$) in the two CID profiles do not match exactly because, due to experimental difficulties, we were unable to perform these experiments in sequence, one after another, so the experimental conditions (most likely argon buffer gas pressure) were slightly different.

obtained by protonation of the commercially obtained *N*-acetylglycine. No estimate for the rate coefficient of this reaction could be obtained. Equivalent gas-phase reactions to form dipeptides from amino acids by ion–molecule reactions have been observed before,[3] but what is far more interesting here is that in our experiment the formation of the peptide bond is observed in conjunction with the synthesis of the amino acid (in this case glycine).

Conclusions

The protonation of hydroxylamine using CH_5^+ yields two isomers, NH_3OH^+ and higher energy $NH_2OH_2^+$. The formation of $GlyH^+$ and $AlaH^+$ (reactions 2–4) occurs upon insertion of the NH_2 group into a C–H bond and concomitant cleavage of the N–O bond; a water molecule leaves the system. The barrier to the insertion and the product is lower on the β-AlaH$^+$ pathway compared to that of the α-form; i.e., both kinetics and thermodynamics favor the formation of β-AlaH$^+$. The reason for this preference is the more efficient H bonding in the transition-state structure and in the product on the β-pathway.

The experimental evidence shows that protonated amino acids glycine and β-alanine are formed by the reaction of protonated hydroxylamine and the corresponding carboxylic acids, acetic and propanoic. Protonated amino acids are likely formed from the more energetic form of protonated hydroxylamine, NH_2-OH_2^+, while the lower energy form NH_3OH^+ only forms clusters with carboxylic acids.

Both acetic acid[32] and glycine[33] have been detected in one core, known as the "large molecule heimat" (LMH) source

(32) Mehringer, D. M.; Snyder, L. E.; Miao, Y. *Astrophys. J. Lett.* **1997**, *480*, L71.
(33) Kuan, Y.-J.; Charnley, S. B.; Huang, H.-C.; Tseng, W.-L.; Kisiel, Z. *Astrophys. J.* **2003**, *593*, 848.

within the giant molecular cloud complex Sagittarius B2 (although the detection of glycine has been disputed);[34] formation of acetic acid and other complex oxygenated molecules in this source is explicable by gas-phase chemistry involving evaporation of dust grain mantles.[35] There is a very interesting possibility that creation of acetic acid by the reaction of ketene and water is catalyzed not by another gas-phase water molecule but by a water molecule in the ice on the dust grain. Water ice has recently been shown to catalyze proton transport reactions at low temperatures (10−70 K),[36] which is similar to the environment of a molecular cloud. This could make the reaction of ketene and water[1] a significant source of carboxylic acids

around dust grains. Glycine production in the LMH source would be fully consistent with such a model, especially given the proposed presence of NH_2OH on these (evaporating) dust grain mantles,[37] and this is also the most probable source for interstellar detection of propanoic acid and therefore, we suggest, β-alanine.

Supporting Information Available: Gaussian03 archive files (i.e., Cartesian coordinates and electronic energies) and thermochemical information for all structures reported. This material is available free of charge via the Internet at http://pubs.acs.org.

JA068725B

(34) Snyder, L. E.; Lovas, F. J.; Hollis, J. M.; Friedel, D. N.; Jewell, P. R.; Remijan, A.; Ilyushin, J. J.; Alekseev, E. A.; Dyubko, S. F. *Astrophys. J.* **2005**, *619*, 914.
(35) Rodgers, S. D.; Charnley, S. B. *Astrophys. J.* **2001**, *546*, 324.
(36) Duvernay, F.; Chiavassa, T.; Borget, F.; Aycard, J.-P. *J. Phys. Chem. A* **2005**, *109*, 603.
(37) Charnley, S. B.; Rodgers, S. D.; Ehrenfreund, P. *Astron. Astrophys.* **2001**, *378*, 1024.